In vivo burn imaging using Mueller optical coherence tomography

Miloš Todorović, [1,2] Shuliang Jiao, [1,3] Jun Ai, [1] David Pereda-Cubián, [1,4] George Stoica, [5] and Lihong V. Wang [1,6*]

[1]*Department of Biomedical Engineering, Texas A&M University, College Station, TX 77843-3120*
[2]*Current address: General Electric Global Research Center, K1 5C36, 1 Research Circle, Niskayuna, NY 12309*
[3]*Current address: Bascom Palmer Eye Institute, University of Miami, 206 McKnight Building (Vision Research), 1638 N.W. 10th Avenue, Miami, FL 33136*
[4]*Current address: Applied Optics Techniques Group, TEISA Department, University of Cantabria, Av. Castros s/n, 39005 Santander, Spain*
[5]*Department of Pathobiology, Texas A&M University, College Station, TX 77843-5547*
[6]*Current address: Optical Imaging Laboratory, Department of Biomedical Engineering, Washington University in St. Louis, Campus Box 1097, One Brookings Drive, St. Louis, MO 63130-4899*
*Corresponding author: LHWang@biomed.wustl.edu

Abstract: We report on the use of a high-speed, fiber-based Mueller-matrix optical coherence tomography system with continuous source-polarization modulation for *in vivo* burn depth evaluation and healing monitoring. A homemade hand-held probe with integrated optical scanning and beam delivering optics was coupled in the sample arm. *In vivo* burn imaging was demonstrated on porcine skin at different stages of the wound healing process, where porcine skin was used because of its similarity to the human skin. Thermally damaged region was clearly localized in the depth-resolved phase retardation image extracted from the measured Jones matrix. The burn areas in the OCT images agreed well with the histology. By using a decomposition algorithm developed by our group, we also mapped the local birefringence of the skin. The experimental results demonstrate the system's potential for *in vivo* burn-depth determination.

OCIS codes: (170.1650) Coherence imaging; (170.3880) Medical and biological imaging; (170.4500) Optical coherence tomography; (260.1440) Birefringence; (260.5430) Polarization; (290.7050) Turbid media.

_____

References and links

1. American Burn Association, "Burn Incidence and Treatment in the US: 2000 Fact Sheet," (2000), http://www.ameriburn.org/resources_factsheet.php.
2. R. S. Cotran, V. Kumar, and S. L. Robbins, *Robbins Pathologic bases of disease* (W.B. Saunders Co., Philadelphia, PA, 1999).
3. R. M. Johnson and R. Richards, "Partial-thickness burns: identification and management," Advances in skin & wound care **16**, 178-187 (2003).
4. J. F. deBoer, T. E. Milner, M. J. C. vanGemert, and J. S. Nelson, "Two-dimensional birefringence imaging in biological tissue by polarization-sensitive optical coherence tomography," Opt. Lett. **22**, 934-936 (1997).
5. M. R. Hee, D. Huang, E. A. Swanson, and J. G. Fujimoto, "Polarization-Sensitive Low-Coherence Reflectometer for Birefringence Characterization and Ranging," J. Opt. Soc. Am. B **9**, 903-908 (1992).
6. J. F. deBoer, S. M. Srinivas, A. Malekafzali, Z. Chen, and J. S. Nelson, "Imaging thermally damaged tissue by polarization sensitive optical coherence tomography," Opt. Express **3**, 212-218 (1998).
7. S. L. Jiao, W. Yu, G. Stoica, and L. H. V. Wang, "Contrast mechanisms in polarization-sensitive Mueller-matrix optical coherence tomography and application in burn imaging," Appl. Opt. **42**, 5191-5197 (2003).
8. B. H. Park, C. Saxer, S. M. Srinivas, J. S. Nelson, and J. F. deBoer, "In vivo burn depth determination by high-speed fiber-based polarization sensitive optical coherence tomography," J. Biomed. Opt. **6**, 474-479 (2001).
9. S. M. Srinivas, J. F. deBoer, B. H. Park, K. Keikhanzadeh, H. L. Huang, J. Zhang, W. Q. Jung, Z. Chen, and J. S. Nelson, "Determination of burn depth by polarization-sensitive optical coherence tomography," J. Biomed. Opt. **9**, 207-212 (2004).

10. M. C. Pierce, R. L. Sheridan, B. H. Park, B. Cense, and J. F. deBoer, "Collagen denaturation can be quantified in burned human skin using polarization-sensitive optical coherence tomography," Burns **30**, 511-517 (2004).
11. G. Yao and L. V. Wang, "Two-dimensional depth-resolved Mueller matrix characterization of biological tissue by optical coherence tomography," Opt. Lett. **24**, 537-539 (1999).
12. S. L. Jiao, M. Todorović, G. Stoica, and L. H. V. Wang, "Fiber-based polarization-sensitive Mueller matrix optical coherence tomography with continuous source polarization modulation," Appl. Opt. **44**, 5463-5467 (2005).
13. G. J. Tearney, B. E. Bouma, and J. G. Fujimoto, "High-speed phase- and group-delay scanning with a grating-based phase control delay line," Opt. Lett. **22**, 1811-1813 (1997).
14. United States National Institutes of Health, "Guide for the care and use of laboratory animals," (US Goverment Printing Office, Washington DC, 1985), NIH Publication No. 86-23.
15. M. Todorović, S. L. Jiao, and L. V. Wang, "Determination of local polarization properties of biological samples in the presence of diattenuation by use of Mueller optical coherence tomography," Opt. Lett. **29**, 2402-2404 (2004).
16. M. J. Escamez, M. Garcia, F. Larcher, A. Meana, E. Munoz, J. L. Jorcano, and M. Del Rio, "An In Vivo Model of Wound Healing in Genetically Modified Skin-Humanized Mice," J. Investig. Dermatol. **123**, 1182-1191 (2004).

1. Introduction

The National Health Interview Survey (NHIS) estimates that there are more than 1.1 million burn injuries per year in the United States [1]. Approximately 45,000 of these injuries require hospitalization, and roughly 4,500 people die from burn injuries annually. In addition, up to 10,000 people in the United States die every year from burn-related infections.

A burn is defined as tissue damage caused by a variety of agents, such as heat, chemicals, electricity, sunlight, and nuclear radiation. The clinical significance of a burn depends on, among other things, its depth [2]. In superficial burns, the dermis is spared and often the epidermis, though devitalized, still exists. Superficial partial-thickness burns extend through the epidermis into the papillary layer of the dermis. Deep partial-thickness burns affect the reticular layer of the dermis. Finally, full-thickness burns extend through the epidermis and dermis into the subcutaneous tissue layer [3].

Without a biopsy, it is difficult to determine the depth of a burn. Currently such determinations are generally made by professionals who must make an educated guess after observing the injury for several days. A non-invasive imaging modality for evaluating burn depth would be of great help to physicians and patients. One such potential technique is polarization-sensitive optical coherence tomography (PS-OCT) [4, 5], which uses changes in the polarization properties of thermally damaged tissue to assess the extent of a burn injury. De Boer et al. first suggested the use of PS-OCT for imaging thermally damaged tissue in [6]. Their *ex vivo* study of burn injuries in porcine skin showed changes in the amount of birefringence, which the authors correctly attributed to collagen denaturation resulting from the exposure to high heat. Several *ex* and *in vivo* studies [7-9] have shown the potential of PS-OCT in detecting changes in rat skin induced by thermal injury. Finally, an *ex vivo* study showed the applicability of this technology in human skin burn assessment [10]. All of these studies focus on the determination of the burn extent immediately following the injury. From the physician's stand point it is equally important to be able to monitor the healing process several weeks post injury as it can reveal potential problems preventing the spontaneous closing of the wound from surviving epithelium, thus indicating the need for skin grafting [8].

As a branch of PS-OCT, Mueller-matrix OCT [11] can completely characterize the polarization properties of a sample by measuring the depth-resolved Mueller matrix. Recently, a system with a single light source and continuous modulation of the source polarization was reported by our group for the acquisition of depth-resolved Jones matrix of biological samples [12]. Here in a further extension of the earlier work, a new, high-speed, fiber-based Mueller-matrix OCT system with continuous source-polarization modulation was developed for burn depth evaluation. The system is capable of real-time imaging (8 frames per second, 200 A-scans per frame). The applicability of the system for burn depth determination is demonstrated here by imaging the porcine skin *in vivo*. The results showing the map of the local

birefringence of the *intravital* ear skin are presented. Also, the applicability of the system for healing monitoring is demonstrated.

2. Materials and methods

OCT system

The schematic of the high-speed, continuously source-polarization modulated Mueller-matrix OCT system is shown in Fig. 1. Light from a broadband super-luminescent diode light source (λ_0=1.3 µm, FWHM-BW=60 nm, output power 10 mW, Superlum, Moscow, Russia) is vertically polarized. A polarization modulator (Conoptics; fast axis at 45°) continuously modulates the source-polarization state with a 140 kHz sinusoidal waveform to ensure that multiple cycles of polarization states are applied to each segment of a depth scan (A-scan). The reference arm and the sample arm are composed of single-mode optical fibers. A linear polarizer, oriented at −45°, is placed before the entrance of the single mode optical fiber in the reference arm to control the reference light polarization state. A grating-based rapid scanning optical delay (RSOD) line [13] is used for longitudinal scanning. A collimating lens, galvanometer scanner and focusing lens in the sample arm are integrated into a hand-held probe. Two BK7 prisms are used in the sample arm for dispersion compensation. The combined sample and reference light is split into horizontal and vertical polarization components by a polarizing beam splitter and detected by two photodiodes, respectively.

The details of the algorithm for extracting the round-trip Jones matrix from the orthogonal intensity measurements appear in our previous paper [12]. Following the same derivation with modifications necessitated by changes in the configuration of the sample arm (galvanometer-based hand-held probe) and the reference arm (RSOD), we arrive at the equations for calculating the Jones matrix elements:

$$
\begin{aligned}
J_{11} &= 0.5\left[I_{aH}(\omega_c) - I_{aH}(\omega_b)\left(1 + \mathbf{J}_0(A)\right)/\mathbf{J}_1(A)\right]/\left|E_r\right| \\
J_{12} &= 0.5\left[I_{aH}(\omega_c) + I_{aH}(\omega_b)\left(1 - \mathbf{J}_0(A)\right)/\mathbf{J}_1(A)\right]/\left|E_r\right| \\
J_{21} &= J_{12} \\
J_{12} &= -0.5\left[I_{aV}(\omega_c) + I_{aV}(\omega_b)\left(1 - \mathbf{J}_0(A)\right)/\mathbf{J}_1(A)\right]/\left|E_r\right|
\end{aligned}
\tag{1}
$$

In the above equations, indices H and V denote components detected by the horizontal and vertical polarization detectors, respectively; I_{aH} and I_{aV} are the analytic signals of the interference signal intensities at the corresponding polarization states; E_r is the amplitude of the reference electric field; $\mathbf{J}_0(A)$ and $\mathbf{J}_1(A)$ are the 0th and 1st order Bessel functions of the first kind, respectively; A is the amplitude of the modulation waveform; ω_c ($\omega_c t = k\Delta z$) is the carrier angular frequency where k is the central wave number and Δz is the optical path length difference between the reference and sample arms; and ω_b ($\omega_b t = \omega_m t - k\Delta z$) is the beating angular frequency where ω_m is the modulation angular frequency.

Given the band-limited equipment (filters and data acquisition board), we selected the components of the interference signals at the lowest frequencies to calculate the Jones matrix elements. Those are the terms at the carrier frequency (90 kHz) and the beating frequency (50 kHz). The equations in Eq. (1) were derived under the condition that the phase modulation is continuous and sinusoidal. It is important that the polarization modulator not be saturated at any point. Hence, amplitude A in the above equations must be selected accordingly.
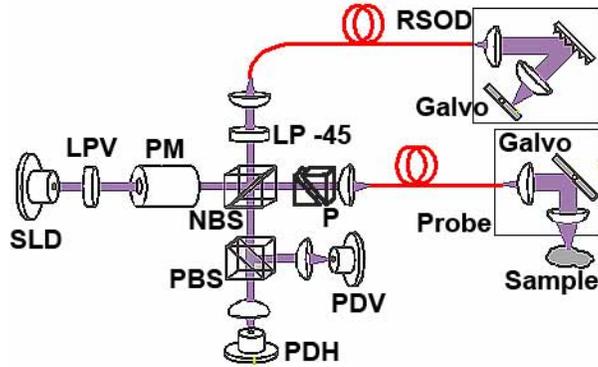
Fig. 1. Schematic of the Mueller PS-OCT system. SLD, super-luminescent diode; PM, polarization modulator; NBS, non-polarizing beam splitter; PBS, polarizing beam splitter; PDH, PDV, photodiodes for horizontal and vertical polarization, respectively; RSOD, rapid scanning optical delay line; LPV, vertical linear polarizer; LP -45, -45° linear polarizer; P, BK7 glass prisms.

Animal studies

All experimental procedures on the pigs were approved by the University Laboratory Animal Care Committee (ULACC) of Texas A&M University and followed the guidelines of the United States National Institutes of Health [14].

The application of the system for *in vivo* burn depth determination was first investigated by imaging porcine (Yorkshire cross, 10 kg body weight) ear skin exposed for 10 seconds to a cauter heated to 150 °C. The entire procedure was performed under anesthesia (preanesthetic xylazine 2.2 mg/kg, intra-muscular (IM) and anesthetic ketamine 40 mg/kg, IM). According to the ULACC approved protocol, the induced burns were treated with topical antibiotic (5%) ointment to protect wounds against bacterial contamination. Upon completion of the OCT imaging, the animal was euthanized with a pentobarbital overdose (100 mg/kg, IM). The excised skin tissue was fixed in a 10% buffered neutral formalin, and the paraffin-embedded tissue was sectioned and stained with hematoxylin and eosin (HE). The stained sections were examined under an Olympus BH-2 light microscope with 4x magnification to evaluate the thermally induced changes.

Following the successful *in vivo* imaging of the porcine ear skin, a time point experiment was performed to investigate the changes of polarization properties of porcine skin from a dorso-lateral site as the skin was healing after a burn injury. Four identical sets of burn injuries, with each set consisting of four burns, were inflicted on the skin. Each set had burns made with the electrical cauter heated to 125 °C and 150 °C, and exposed for 10 and 30 seconds at each temperature. Again, the entire procedure was performed under anesthesia and the induced burns were treated with topical antibiotic ointment to protect wounds against bacterial contamination. The healing progress was observed bi-weekly following the injury. Upon completion of the OCT imaging at each time point, a biopsy was performed. At the end of the eight week period, the animal was euthanized.

3. Results and discussion

We first verified the system's performance by measuring the resolution and sensitivity. The depth resolution depends on the characteristics of the light source and was measured to be 14 µm in air (10 µm in biological tissue assuming an index of refraction of 1.4). This is comparable to the theoretical value of 12.5 µm in air. The resolution was determined by imaging the surface of a glass plate and measuring the full width at half maximum (FWHM) of a representative longitudinal scan (depth scan or A-scan). The sensitivity was measured by

imaging a standard mirror through a set of neutral density filters of known attenuations. The number of filters in the set, and consequently the attenuation, were increased until the mirror surface was indiscernible from noise. The sensitivity was determined to be 78 dB.

The application of the system for *in vivo* burn depth determination was first investigated by imaging burnt porcine ear skin. Fig. 2 shows the OCT intensity (a), integrated (b) and differentiated [15] (c) phase retardation images of the ear skin after burning. The HE stained histology image (d) is included for comparison.

The healthy region of the epidermis, as determined from the differentiated phase retardation image (Fig. 2(c)), has an average birefringence of $3.0\pm0.2\times10^{-4}$ and the healthy dermis exhibits a birefringence of $5.1\pm0.2\times10^{-3}$ (95% confidence intervals). The loss of birefringence is visible in the thermally damaged region in Figs. 2(b) and 2(c) and is likely attributed to the denaturation of collagen-based connective tissue in the dermis. The marked burn areas in the phase retardation images and histology compare well with each other in shape and location. The depth of the burn determined by the OCT system is 0.47 mm, while the depth obtained from the histology is 0.41 mm. This difference in absolute depths can be attributed to tissue shrinkage due to formalin fixation and the fact that the histology cut was performed at a position that might have been slightly different from the one imaged with the OCT system. The birefringence in the burnt area is $2.2\pm0.2\times10^{-4}$ (95% confidence interval). This value is an order of magnitude smaller than the value observed in healthy dermis and is close to the value detected in healthy epidermis. Based on the depth, the burn can be classified as a superficial partial-thickness burn according to the nomenclature presented in the literature [3].
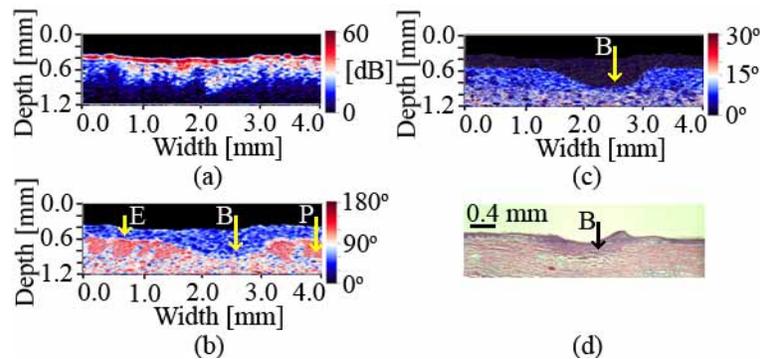

Fig. 2. Intensity (a), integrated (b) and differentiated (c) phase retardation, and HE stained histology (d) images of a burnt porcine ear skin. E – epidermis; P – papillae; B – burn. The burn depth is determined to be 0.47 mm (OCT) and 0.41 mm (histology). The difference in burn depth can be attributed to tissue shrinkage due to formalin fixation.

A time point experiment was designed to investigate the changes that occur in the skin during the post-burn healing. Fig. 3 shows two sets of experimental results for burns inflicted for 30 seconds at 125 °C. The results obtained for burns inflicted at other exposure-time/temperature combinations are similar. The upper row (Figs. 3(a)-3(c)) shows the intensity, phase retardation and HE stained histology images, respectively, of the porcine skin from the dorso-lateral region immediately after burning. Second and third rows (Figs. 3(d)-3(h)) show images of a second burn from the same region (identical exposure time/temperature combination) taken immediately post-burning and after 4 weeks of healing. The location of the burn is clearly identifiable in all phase retardation images. The healing process was completely natural and was not promoted by any ointments. A topical antibiotic was applied to prevent infection.

Comparison of the phase retardation images post-burn and after four weeks of healing shows marked difference in the burnt area. While the damage to the epidermis and dermis is

clearly visible in the fresh burn, the epidermis and the proximal layers of dermis are almost completely healed after four weeks. However, the deeper regions of dermis are still damaged. This is consistent with the nature of the skin regeneration process where the remaining epidermis surrounding the burn will start to proliferate into the burnt region and the epidermis will close within approximately a week [16]. By contrast, collagen fibers in dermis need more time to mature and regain their original matrix organization. The proximal dermis is pulled in towards the center of the wound by the proliferating epidermis and regenerates faster than the distal regions. The structures observed in OCT images correspond well to the structures seen in histological analysis.
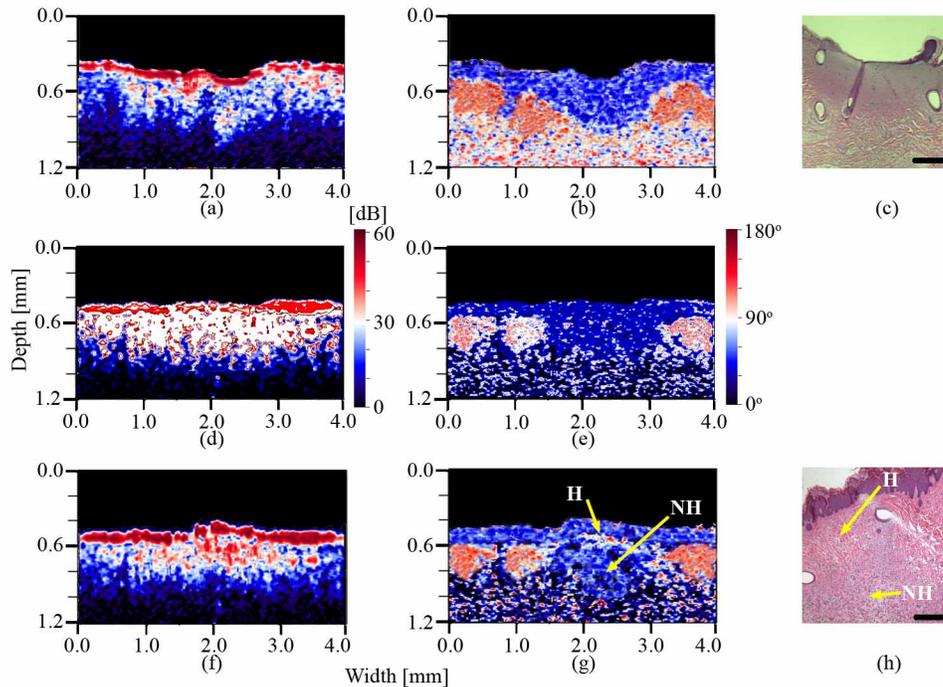

Fig. 3. Intensity (a), phase retardation (b) and HE stained histology (c) images of the burnt porcine dorso-lateral skin immediately following the injury; intensity (d) and phase retardation (e) images of the second burn from the same region immediately post-burning; and the intensity (f), phase retardation (g) and the and HE stained histology (h) images of the second burn after four weeks of healing. H – epidermal and proximal dermal region healed after four weeks; NH – deeper dermal region not healed after four weeks. Vertical and horizontal bars in HE stained histology images represent 0.2 mm.

4. Conclusions

In conclusion, we have presented the use of a new high-speed, fiber-based Mueller-matrix OCT system with continuous source-polarization modulation for *in vivo* burn imaging. For the first time to our knowledge, a map of the local birefringence of *intravital* porcine skin was presented. The system is capable of accurately localizing changes in polarization properties that are due to thermal damage of tissue *in vivo* and, hence, has the potential to aid physicians in determining the extent of burn injuries and subsequent monitoring of the skin regeneration.